

Solvent vapor induced dewetting in diblock copolymer thin films

Juan Peng, Yu Xuan, Hanfu Wang, Binyao Li, Yanchun Han*

State Key Laboratory of Polymer Physics and Chemistry, Changchun Institute of Applied Chemistry, Chinese Academy of Sciences, 5625 Renmin St., Changchun 130022, People's Republic of China

Received 23 September 2004; received in revised form 26 January 2005; accepted 2 May 2005

Available online 8 June 2005

Abstract

The dewetting pattern development of thin film of poly(styrene)-*block*-poly(methyl methacrylate) (PS-*b*-PMMA) diblock copolymer has been studied after ‘annealing’ in the PMMA block selective solvent vapor. Initially, typical circular dewetted holes are observed. Further annealing, however, results in the formation of fractal-like holes. The heterogeneous stress induced by the residual solvent remaining in the film after spin-coating induces the anisotropy of the polymer mobility during the annealing process, which triggers the formation of the intriguing surface patterns.

© 2005 Elsevier Ltd. All rights reserved.

Keywords: Dewetting; Diblock copolymers; Fractal-like holes

1. Introduction

The dewetting of thin polymer films has been a much-studied problem in recent years due to its theoretical and technological importance [1–3]. It is known that a liquid film on a substrate is non-wetting if its spreading coefficient, $S = \gamma_{sv} - (\gamma_{sl} + \gamma_{lv})$, is negative [4]. Here, γ_{sv} is the interfacial tension between the solid substrate and the vapor phase, γ_{sl} is the interfacial tension between the substrate and the liquid, and γ_{lv} is that of the liquid/vapor interface. Recently it was shown that one might consider the free energy U to gain some insight into the nature of pattern formation. When non-retarded van der Waals interactions are dominant, the free energy U per unit area of a film of thickness h is given by

$$U(h) = -\frac{A}{12\pi h^2} \quad (1)$$

Here, A is the difference between the liquid–liquid and solid–solid Hamaker constants [5]. If A is positive, the van der Waals interactions thin the film, enhancing surface fluctuations, and after a characteristic time, the film ruptures

[6,7]. Two possible rupture mechanisms are discussed: (i) heterogeneous hole nucleation due to defects or impurities in the film, and (ii) spontaneous film rupture under the influence of long-range interactions (such as the van der Waals force), known as spinodal dewetting.

An extremely good model system for such studies is that of polystyrene. Reiter [8] has characterized the progression of dewetting from early to complete dewetting using polystyrene films heated above its glass transition temperature (T_g). First, the films break up thus creating randomly distributed holes. Second, the holes then grow and form rims ahead of them, which finally contact each other creating cellular structures. Third, the resulting ribbons are unstable and decay into droplets.

Research on this topic has, for the most part, been exclusively devoted to the dewetting of simple polymeric fluids from solid and from liquid substrates [8–21]. Usually, the dewetting processes are induced by annealing above the T_g of polymers. Little is understood about the dewetting of structured fluids such as block copolymers [22–24], especially the dewetting of block copolymers induced by solvent vapor. In the present work, we investigated the time evolution of the dewetted hole pattern in thin films of a symmetric diblock copolymer poly(styrene-*b*-methyl methacrylate) (PS-*b*-PMMA) during solvent vapor treatment. The solvent used is a selective solvent for PMMA and non-selective for PS. Thin films (~ 22 nm) of this copolymer are shown to undergo dewetting via a nucleation

* Corresponding author. Tel.: +86 431 5262175; fax: +86 431 5262126.
E-mail address: yehan@ciac.jl.cn (Y. Han).

and growth mechanism. We show that ordinary circular holes form at the initial stage of annealing. Further annealing, however, leads to the formation of fractal holes. A small amount of residual toluene solvent remaining in the film after spin-coating induces the anisotropy of the polymer mobility during the annealing process, which triggers the formation of the intriguing surface patterns. This, to our knowledge, appears to be the first time to investigate the development of dewetted fractal holes in block copolymer thin films induced by solvent vapor annealing.

2. Experimental details

2.1. Sample preparation

PS-*b*-PMMA ($M_{PS} = 133,000$, $M_{PMMA} = 130,000$, $M_w/M_n = 1.07$, $L_0 = 90$ nm) was purchased from Polymer Source, Inc. The diblock copolymer was dissolved in toluene with typical concentration of 0.5 wt%. Thin polymer films (~ 22 nm) were then prepared by spin-coating the toluene solution onto the silicon oxide (~ 2 nm-thick from ellipsometry) at 2000 rpm for 30 s. Prior to spin-coating, the wafers were cleaned with a 70/30 v/v solution of 98% H_2SO_4 /30% H_2O_2 at 80 °C for 30 min, and then thoroughly rinsed with deionized water and dried. Film thickness was measured by an ellipsometry (AUDEL-III, Xi'an, China). Without removing the residual solvent, the samples were exposed to the saturated acetone vapor in a closed vessel. All experiments were performed at room temperature. After solvent treatment from 1 to 58 h, the samples were removed from the vessel quickly for fast drying.

The minimal amount of residual solvent that is needed to trigger the fractal-like hole formation is determined by the following method. To avoid any experimental uncertainty, the samples for the determination of the amount of residual solvent were cut from the same specimen as that used for acetone vapor annealing. The film specimens were pre-annealed with different time to reduce the residual solvent content to different degree and then the film thickness was measured by ellipsometry. Subsequently, the film was annealed in acetone vapor to see if the fractal holes can be produced. When the fractal holes cannot be observed any more, the sample was annealed at 50 °C for 3 day to remove the residual solvent completely and its thickness was measured again. The thickness reduction can be determined which is related to the minimal amount of residual solvent that is needed to trigger the fractal-like hole formation.

2.2. Atomic force microscopy (AFM) characterization

The surface morphology was observed by a commercial atomic force microscopy (AFM), using a SPA300HV with a SPI3800N controller (Seiko Instruments Inc., Japan) in the

tapping mode (set point ratio ≈ 0.90). Silicon tips on cantilevers (resonance frequency 70 kHz) with spring constant 2 N/m were used. The scan rate was in the range 1.0–2.0 Hz.

2.3. Optical microscopy (OM) characterization

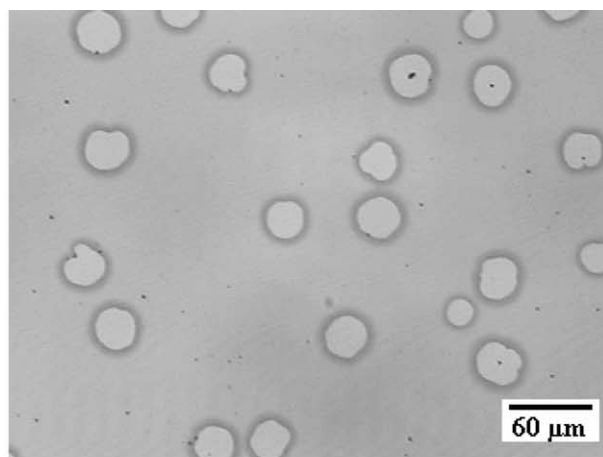
Optical microscopy (OM) measurements were performed with a Leica optical microscopy (Leica Microsystems, Germany) in reflection mode with a CCD camera attachment.

3. Results and discussion

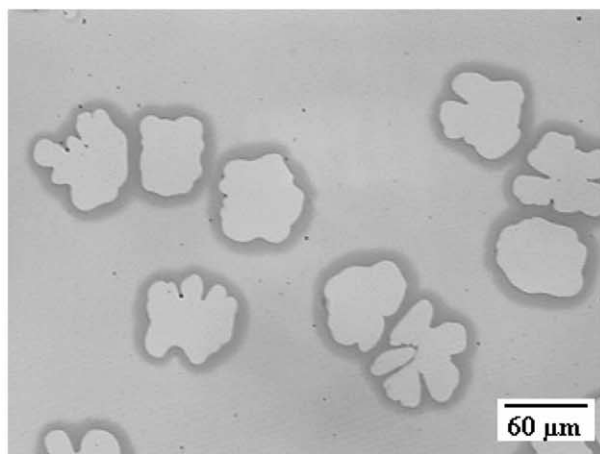
The as-cast PS-*b*-PMMA thin films are observed to be featureless in optical microscope, since they are kinetically trapped in disordered state due to the spin-coating process. At the initial stage of acetone vapor annealing (6 h), ordinary circular holes occur randomly distributed in the film (Fig. 1(a)). Further annealing to 9.5 h, however, leads to the formation of fractal-like holes (Fig. 1(b)), which grow in size with annealing time as shown in Fig. 1(c). The typical size of fully grown fractal holes exceeds 150 μm , which is quite large.

AFM measurement was carried out in order to obtain the accurate information on the profile of the film. Fig. 2(a) and (b) show the AFM height images and the cross-sectional height profiles of PS-*b*-PMMA thin films after annealing in acetone vapor for different times. As expected, circular holes are formed at the initial stage of annealing (Fig. 2(a)). Interestingly, a dewetted fractal hole starts to develop at this time. Although we observe the fractal-like hole in Fig. 2(a), the number density of the fractal hole is quite small at this annealing time. The cross-sectional height profile in Fig. 2(a) shows that a rim forms at the edge of the hole and the hole depth is 13 nm. Note that the initial thickness of the film is 22 nm, a layer of approximately 9 nm is left on the silicon substrate. As time lapses, the fractal holes are developed (Fig. 2(b)). The line profile implies the depth of the fractal hole is about 42 nm and the left polymer layer remains on the substrate. The structure of the copolymer film left behind in dewetted holes was also investigated. Fig. 2(c) shows an ultrathin film of the copolymer covers the surface with some round-shaped objects on it. It resembles the autophobic dewetting which has been reported on thin film of some block copolymer systems [23,25]. We attribute it to dense brush layer of ordered copolymer due to the strong attraction between PMMA chains and the native silicon oxide layer on the substrate.

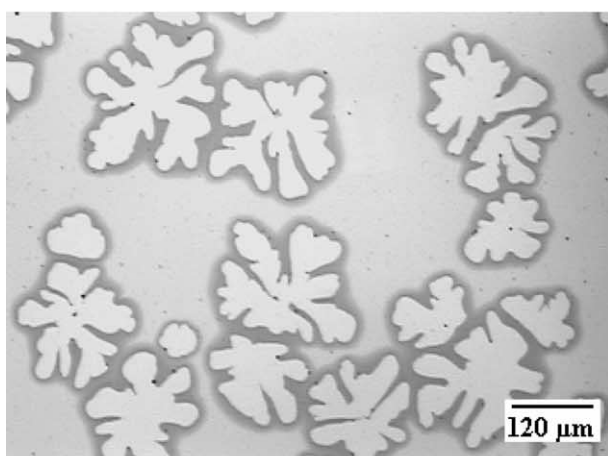
Fractals in our system are quite similar in shape to non-equilibrium patterns observed in other systems, such as dendritic crystallization, electrodeposition, viscous fingering, and dielectric breakdown [26,27], etc. As a result, we performed the fractal dimension analysis for an isolated fully developed hole by using the box count method [26,27],



(a)



(b)



(c)

Fig. 1. Optical micrographs in reflection mode for PS-*b*-PMMA thin films with $t_0 \sim 1/4L_0$ after solvent annealing in acetone vapor for (a) 6 h, (b) 9.5 h, and (c) 26 h, respectively.

and the results are shown in Fig. 3(a). The fractal dimension d_f of the hole can be obtained from the scaling relationship of $N(l) \sim l^{-d_f}$, where $N(l)$ is the number of boxes of size l that contain at least part of the hole region. From the slope in Fig. 3(a), $d_f = 1.67$ was obtained. Analysis of many such holes yielded nearly the same fractal dimension in exact agreement with the theoretical result of Muthukumar [28], $d_f = (d^2 + 1)/(d + 1)$, where $d = 2$ is the space dimension. This result is also consistent with the results reported by Lee et al. [29,30] and Koneripalli et al. [31], which are quite informative to our study.

Image analysis was then performed for the dewetted films in order to obtain quantitative information on the growth process of fractal holes. Fig. 3(b) shows the time evolution of the fractal dimensions of the fractal holes during acetone vapor annealing. It can be seen the fractal dimension gradually increases from 1.14 at short annealing time to 1.67 at long annealing time. On an extended acetone vapor treatment, the fractal holes were destroyed and developed into the classic late-stage dewetted droplet pattern.

Lee et al. [29,30] prepared a symmetric PS-P2VP diblock copolymer thin film with an initial thickness of $1.5L_0 < t_0 < 3.5L_0$. Subsequent thermal annealing led to the development of dual morphology of islands and fractal holes similar in form to ours. They attributed it to the kinetically trapped metastable structure induced by a high-boiling residual solvent. Koneripalli et al. [31] prepared a 3/2 bilayer film of a symmetric PS-P2VP diblock copolymer with a thickness of $1.45L_0$ by confinement technique followed by thermal annealing. Subsequent annealing after removing the confinement layer also led to the development of fractal holes. They attributed this fractal hole formation, which is governed by the Laplace equation with moving boundary conditions, to the heterogeneous nucleation by tiny dust particles in laterally strained lamellae. The important differences between the present work and their works are that the PS-*b*-PMMA films are very thin ($\sim 1/4L_0$) and treated by solvent annealing instead of thermal annealing. Thus the fractal hole in our system has only two flat regions of different heights without hole-in-hole structure.

Before interpreting the fractal structure formation, we would discuss why the PS-*b*-PMMA thin film dewetted the silicon surface when exposed to acetone vapor. Usually, the dewetting processes are induced by annealing above the T_g of polymers to activate the polymer chains. Diblock copolymer thin films above the bulk order-disorder transition (ODT) temperature exhibit properties similar to those of simple homopolymer liquids. As we know, two factors influence T_g : the interaction with the substrate and the film thickness [32,33]. T_g is low for weak substrate-polymer interaction, and it is high for strong interaction. In this case, exposing the thin films to solvent vapor is qualitatively found to have a similar effect on the microstructure to that of thermal annealing. In a dry state,

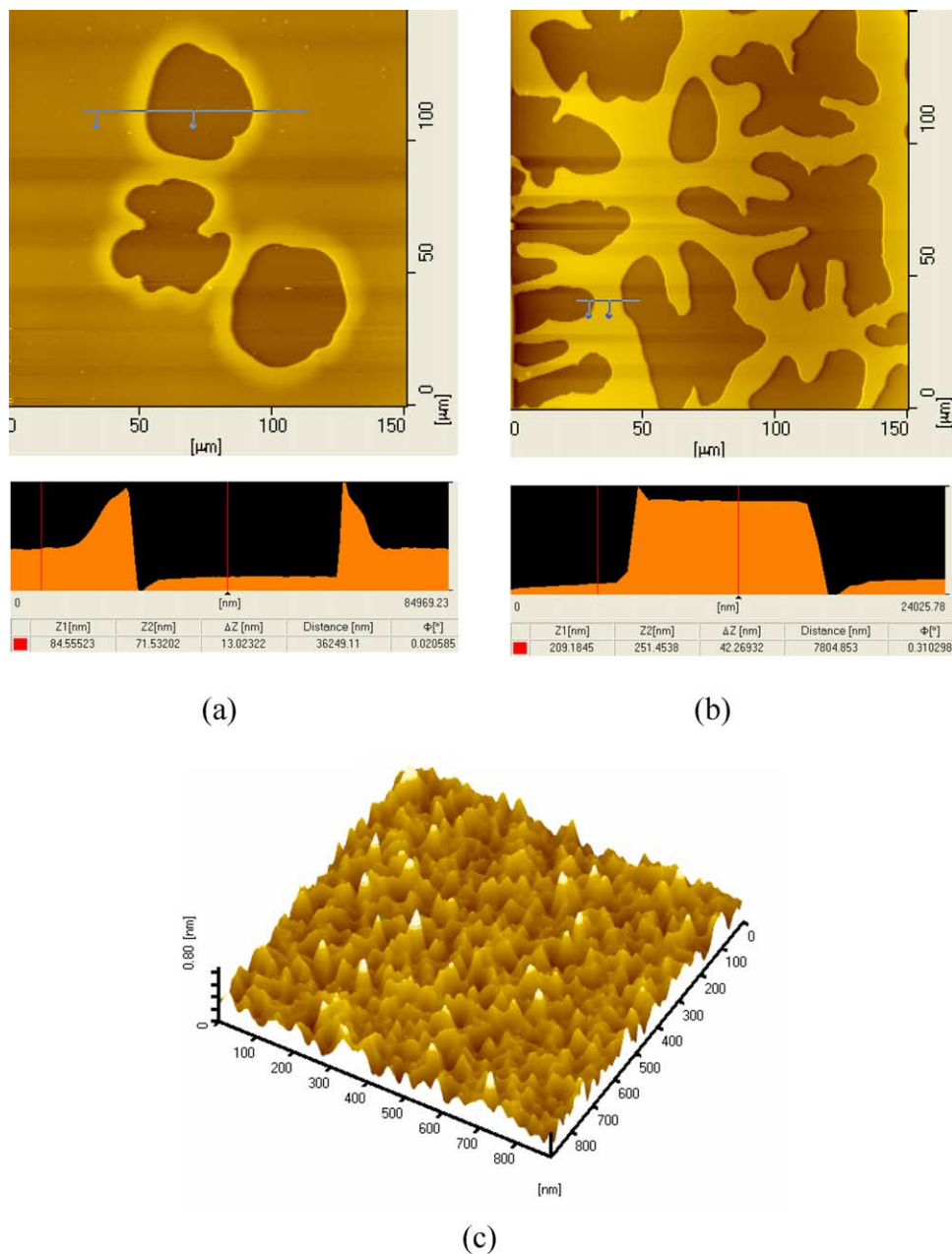


Fig. 2. AFM height images and cross-sectional height profiles of PS-*b*-PMMA thin films after solvent annealing in acetone vapor for (a) 6 h and (b) 26 h, respectively. (c) A 3D AFM height image showing the structure of the copolymer film inside the fractal hole after acetone vapor annealing for 24 h.

the PS-*b*-PMMA exists in the glassy state and exhibits very slow relaxation processes. On exposure to acetone vapor, which is a preferential solvent for PMMA, the PMMA block was swollen and the mobility of the chains was greatly increased. During the initial swelling period, the PS domains remain below their T_g and fixed. After a certain time of exposure to acetone vapor, enough solvent has penetrated to PS domains to allow molecular reconfiguration and stress relaxation, lowering their effect T_g . Therefore, the occurrence of glass transition at the room temperature becomes true [34,35].

In our case, one of the driving forces for the dewetting of

PS-*b*-PMMA films on the silicon oxide is the strong tendency of acetone molecules to attract the PMMA uprising. Previous description [36–38] has shown that when symmetric PS-*b*-PMMA is cast on a Si substrate with a SiO_x surface layer, the PMMA preferentially segregates to the substrate while the PS segregates to the air interface due to the presence of asymmetric boundary condition. On exposure to acetone vapor, a selective solvent for PMMA, it turns into symmetric boundary condition [39, 40]. Solvent vapor molecules have a strong tendency to attract PMMA to maximize the PMMA-solvent contacts. So PMMA is pulled toward the film surface. The movement of

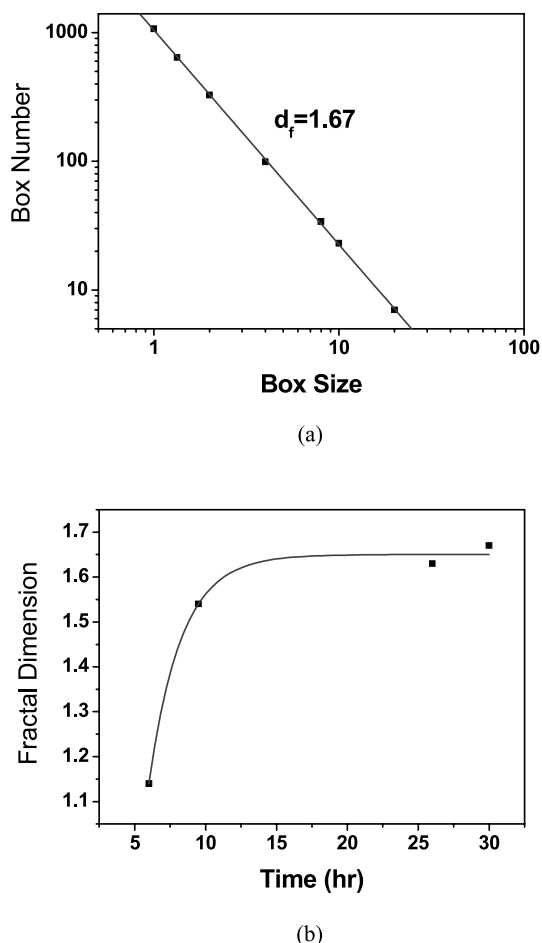


Fig. 3. (a) Analysis of the fractal dimension of a fully developed fractal hole by using the box count method. (b) Time evolution of the fractal dimension of holes in PS-*b*-PMMA films during acetone vapor annealing.

PMMA uprising destabilizes the film and leads to dewetting. To verify this effect, the as-cast samples were also exposed to carbon disulfide (selective for PS) and toluene (slightly selective for PS) vapor, respectively, and the films were stable. It is because that on exposure to PS-selective solvents, the upper boundary condition still favors the PS, and the PS will continue to dominate the upper surface. The solvents disturb the film less and thus no dewetting occurred. Microscopically heterogeneous stress is believed to trigger the formation of fractal holes and the heterogeneity comes from the residual toluene solvent. The residual solvent evaporates and causes small thickness variations, inducing anisotropic stress in the films. At first sight, this idea of a ‘heterogeneous propagation of stress’ does not seem to apply to PS-*b*-PMMA thin films on the silicon substrate because the polymer and the substrate are highly homogeneous. In the absence of acetone, the residual solvent is insignificant because the film is stable. If, however, acetone vapor is present and destabilizes the polymer, heterogeneous stress induced by the residual solvent is amplified and causes the heterogeneous polymer mobility, resulting in the fractal holes. Fig. 4 shows a

schematic of the fractal hole formation in our block copolymer thin film. The as-cast film contains a small amount of solvent (typically below 4%) due to the spin-coating process using the high boiling toluene solvent ($T_b = 110\text{ }^\circ\text{C}$) at a relatively low spinning speed. After the typical circular holes occur during the early stage of dewetting (Fig. 4(a)), the residual toluene solvent gradually causes the anisotropic stress throughout the film, thereby destabilizing an initially uniform front and inducing the heterogeneity of the polymer mobility (Fig. 4(b)). The evolution of the dewetted hole front becomes anisotropic and some spreading front dewets faster than the adjacent regions, forming fractal hole (Fig. 4(c)). Then, the dewetting is towards the ‘fingering’ direction continuously and develops into the fully grown fractal-like holes (Fig. 4(d)). For comparison, we pre-annealed the as-cast specimen at $50\text{ }^\circ\text{C}$ for 15 h in vacuum to reduce the residual solvent content to about 1%. Subsequent annealing in acetone vapor produced much less fractal holes with smaller sizes. We also pre-annealed the thin film at $50\text{ }^\circ\text{C}$ for 3 days in vacuum to remove the residual solvent completely. After annealing in acetone vapor, it was found that the fractal holes disappeared completely. Note that this thermal annealing process could not cause polymer segregation between PS and PMMA blocks, since the glass transition temperatures of both components are far above this temperature. We investigated the surface morphology of the films with or without residual

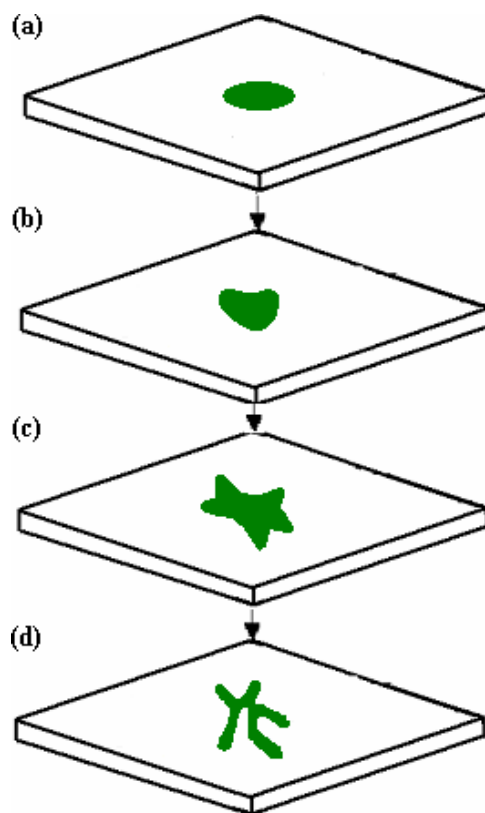


Fig. 4. Schematic of the dewetted fractal hole formation in PS-*b*-PMMA thin films induced by the residual solvent.

solvent before solvent annealing both showed the same disordered wormlike pattern at nanometer scale (not shown here). It revealed that the heterogeneous stress induced by the residual solvent triggered the formation of fractal holes and the decrease of residual solvent content in the film retarded the fractal hole growth. Our further investigations show that when the amount of residual solvent is less than 0.5%, the fractal-like hole will not appear any more.

4. Conclusions

In conclusion, we have investigated the dewetting of fractal holes in symmetric PS-*b*-PMMA diblock copolymer thin films ($t_0 \sim 1/4L_0$) during solvent vapor annealing in acetone. Dewetting at the copolymer surface occurs via a nucleation and growth mechanism. The formation of fractal holes is due to the anisotropy of the polymer mobility induced by the residual toluene solvent. The resulting thin films are believed to be a promising candidate for non-glossy coating materials due to their intriguing self-similar micropatterns.

Acknowledgements

This work is subsidized by the National Natural Science Foundation of China (50125311, 20334010, 20274050, 50290090, 50373041, 20490220), the Ministry of Science and Technology of China (2003CB615601, 2002CCAD4000), the Chinese Academy of Sciences (Distinguished Talents Program, KJCX2-SW-H07) and the Jilin Distinguished Young Scholars Program (20010101).

References

- [1] de Gennes PG. *Rev Mod Phys* 1985;57:827.
- [2] Krausch G. *J Phys Condens Matter* 1997;9:7741.
- [3] Becker J, Grün G, Seemann R, Mantz H, Jacobs K, Mecke KR, et al. *Nat Mater* 2003;2:59.
- [4] Young T. *Philos Trans R Soc London* 1805;95:65.
- [5] Yerushalmi-Rozen R, Klein J, Fetters LJ. *Science* 1994;263:793.
- [6] Vrij A. *Discuss Faraday Soc* 1967;42:23.
- [7] Scheludko A. *Adv Colloid Interface Sci* 1967;1:391.
- [8] Reiter G. *Phys Rev Lett* 1992;68:75.
- [9] Neto C, Jacobs K, Seemann R, Blossey R, Becker J, Grün G. *J Phys Condens Matter* 2003;15:S421.
- [10] Brochard-Wyart F, Martin P, Redon C. *Langmuir* 1993;9:3682.
- [11] Shull KR, Karis TE. *Langmuir* 1994;10:334.
- [12] Faldi A, Composto RJ, Winey KI. *Langmuir* 1995;11:4855.
- [13] Lambooy P, Phelan KC, Haugg O, Krausch G. *Phys Rev Lett* 1996;76:1110.
- [14] Du BY, Xie FC, Wang YJ, Yang ZY, Tsui OKC. *Langmuir* 2002;18:8510.
- [15] Xie R, Karim A, Douglas JF, Han CC, Weiss RA. *Phys Rev Lett* 1998;81:1251.
- [16] Sharma A, Khanna R. *Phys Rev Lett* 1998;81:3463.
- [17] Li X, Han YC, An LJ. *Polymer* 2003;44:5833.
- [18] Zhang ZX, Wang Z, Xing RB, Han YC. *Polymer* 2003;44:3737.
- [19] Ashley KM, Meredith JC, Amis E, Raghavan D, Karim A. *Polymer* 2003;44:769.
- [20] Ton-That C, Shard AG, Bradley RH. *Polymer* 2002;43:4973.
- [21] Leonard DN, Spontak RJ, Smith SD, Russell PE. *Polymer* 2002;43:6719.
- [22] Green PF. *J Polym Sci, Part B: Polym Phys* 2003;41:2219.
- [23] Limary R, Green PF. *Macromolecules* 1999;32:8167.
- [24] Limary R, Green PF. *Langmuir* 1999;15:5617.
- [25] Fukunage K, Hashimoto T, Elbs H, Krausch G. *Macromolecules* 2002;35:4406.
- [26] Vicsek T. *Fractal growth phenomena*. Singapore: World Scientific Publishing; 1989. p. 297–324.
- [27] Meakin P. *Fractal, scaling and growth far from equilibrium*. New York: Cambridge University Press; 1998.
- [28] Muthukumar M. *Phys Rev Lett* 1983;50:839.
- [29] Lee SH, Kang H, Cho J, Kim YS, Char K. *Macromolecules* 2001;34:8405.
- [30] Lee SH, Kang H, Kim YS, Char K. *Macromolecules* 2003;36:4907.
- [31] Koneripalli N, Bates FS, Fredrickson GH. *Phys Rev Lett* 1998;81:1861.
- [32] van Zanten JH, Wallace WE, Wu W. *Phys Rev E* 1996;53:2053.
- [33] Forrest JA, Dalnoki-Veress K, Stevens JR, Dutcher JR. *Phys Rev Lett* 1996;77:2002.
- [34] Leibler L, Sekimoto K. *Macromolecules* 1993;26:6937.
- [35] Albalak RJ, Capel MS, Thomas EL. *Polymer* 1998;39:1647.
- [36] Green PF, Christenson TM, Russell TP. *Macromolecules* 1991;24:252.
- [37] Anastasiadis SH, Russell TP, Satija SK, Majkrzak CF. *Phys Rev Lett* 1989;62:1852.
- [38] Russell TP, Coulon G, Deline VR, Miller DC. *Macromolecules* 1989;22:4600.
- [39] Peng J, Xuan Y, Wang HF, Yang YM, Li BY, Han YC. *J Chem Phys* 2004;120:11163.
- [40] Xuan Y, Peng J, Cui L, Han YC. *Macromolecules* 2004;37:7301.